geoconvention
Calgary • Canada • May 11-13 2026

A Seismic–CSEM Workflow for CO_2 Plume Monitoring: Quantifying Uncertainties in Probabilistic Geometry Reconstruction and Deterministic Saturation Imaging

Vahid Entezar-Saadat[1], Alison Malcolm[1], Colin Farquharson[1]
[1]Memorial University of Newfoundland

Summary

We present a two-stage workflow for CO_2 plume characterization that combines probabilistic full-waveform seismic inversion (FWI) with deterministic controlled-source electromagnetic (CSEM) inversion. In the first stage, we use seismic FWI with Bayesian sampling to estimate the posterior distribution of plume geometry and porosity for a homogeneous reservoir. To make the sampling problem tractable, the boundary is parameterized sparsely and sampled using Markov chain Monte Carlo (MCMC), yielding posterior uncertainty estimates for the plume extent and porosity directly from the ensemble of admissible models. In the second stage, we constrain the seismic-derived porosity and geometry and perform a CSEM inversion using a minimum-structure, nonlinear conjugate gradient (NLCG) inversion to reconstruct the internal fluid-saturation distribution, to which seismic sensitivity is limited. By restricting the CSEM inversion to the seismically inferred plume region and using the boundary as a structural constraint, the electromagnetic problem becomes better posed. Synthetic experiments using a simplified representation of the Johansen formation in the North Sea demonstrate that the proposed two-stage approach can recover the plume geometry and porosity with quantified uncertainty and improve saturation imaging within the plume.

Method

Because injected CO_2 is less dense than the formation brine, it migrates upward until it encounters the top seal (Ozah et al., 2005). We therefore assume that the upper boundary of the plume coincides with the reservoir top and that it can move only laterally along this interface. The lower boundary of the plume is represented by two control nodes with unknown (x, z) coordinates, allowing the plume thickness and shape to vary while preserving geological realism.

We use seismic FWI (Peter et al., 2011) to estimate the CO_2 plume geometry and homogeneous porosity ($\emptyset$) with a parameter vector $\boldsymbol{m}_s(x, z, \emptyset)$, and seek models that are consistent with the observed seismic dataset $\mathbf{d}_s^{obs}$. In a Bayesian setting, inference is expressed in terms of the posterior density (Mosegaard and Tarantola,1995),

$$p(\boldsymbol{m}_s(x,z,\emptyset)|\boldsymbol{d}_s^{obs}) \propto p\left(\boldsymbol{d}_s^{obs}\middle|\boldsymbol{m}_s(x,z,\emptyset)\right) p(\boldsymbol{m}_s(x,z,\emptyset)) \quad (1)$$

where $p(\boldsymbol{m}_s)$ includes prior constraints, and $p\left(\boldsymbol{d}_s^{obs}\middle|\boldsymbol{m}_s\right)$ measures how well a proposed plume model fits the seismic observations via forward simulation. Our prior is implemented as uniform bounds and feasibility checks on plausible geological geometry.

Although seismic velocity is linked to saturation via rock physics, Gassmann fluid substitution (Gassmann, 1951) indicates that V_p is nearly independent of CO_2 saturation beyond ~15%. Thus,

we assume fixed in-plume CO_2 saturation ($S_{CO_2} > 0.15$). We sample the posterior using a Metropolis–Hastings Markov chain algorithm (Metropolis et al., 1953; Hastings, 1970).

After the seismic Bayesian stage provides estimates of the plume boundary and porosity, we freeze the geometry and porosity and restrict the CSEM inversion to the plume interior. The unknown in this second stage is a discretized CO_2 saturation model ($\boldsymbol{m}_{em}(\boldsymbol{S}_{CO2})$). To predict CSEM responses, we map saturation to resistivity using Archie's equation (Archie, 2003) and then compute synthetic CSEM data using forward modeling. For CSEM forward responses and sensitivity (Jacobian) calculations, we use the MARE2DEM package (Key, 2016).

We use the NLCG scheme to estimate $\boldsymbol{m}_{em}$ by minimizing a weighted data misfit and regularization term (Mackie and Madden, 1993). Over iterations, the inversion transitions from strongly regularized (stable, smooth) updates to progressively more data-driven ones.

Results

Johansen Formation: Our synthetic model is built for the Johansen Formation along seismic composite line 1 within the merged 3D seismic volume GN10M1 (Sundal et al, 2016).

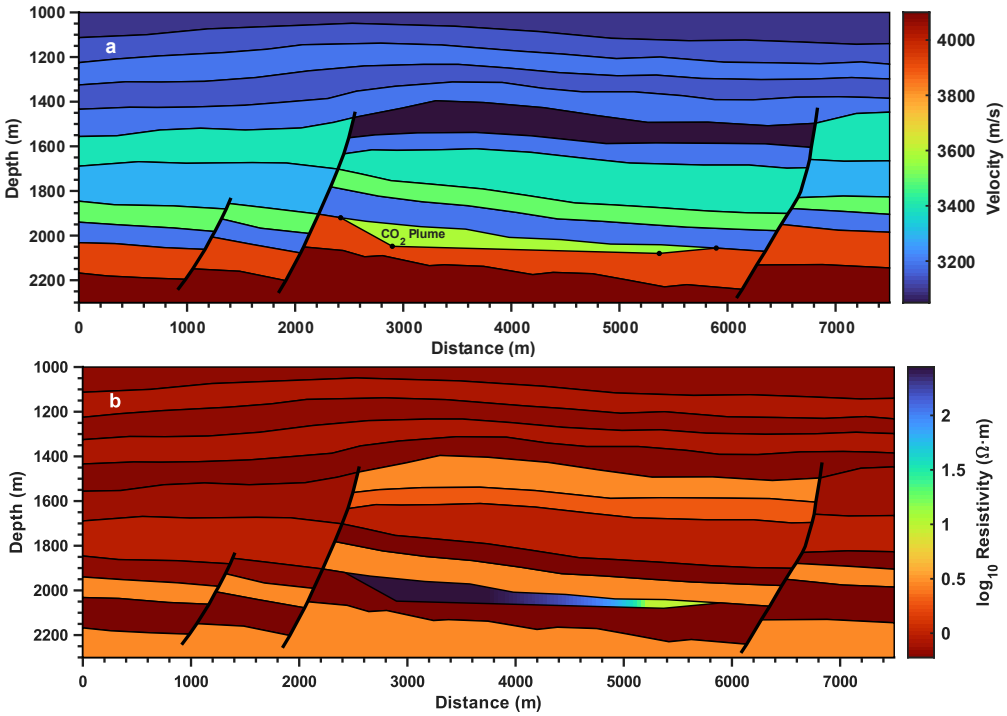


***Figure 1**. **a)** P-wave velocity distribution of the study area. Five surface seismic sources are evenly spaced between 1500 and 6500 m, and ocean-bottom receivers are deployed at 10 m intervals along the full profile. Both horizontal and vertical displacement components are used. Black dots represent the geometry parameters. **b)** Resistivity distribution of the study area. For the CSEM inversion, 11 horizontal electric dipole transmitters (0.01 Hz) are evenly distributed along the profile from 0 to 7500 m. Seafloor receivers are deployed at 400 m spacing between 1400 and 7000 m, providing dense coverage across the target plume interval.*

FWI results: For each parameter set, we generate two-dimensional elastic property models (Figure 1) using Coreform Cubit 2025.8 (Coreform Cubit, 2025). The corresponding seismic responses are simulated using the spectral-element code SPECFEM2D (Peter et al., 2011).

We use a 15 Hz seismic source frequency with a Ricker wavelet. We simulate two chains, each with 5,000 iterations. Figure 2 shows the recovered posterior distributions for each parameter.

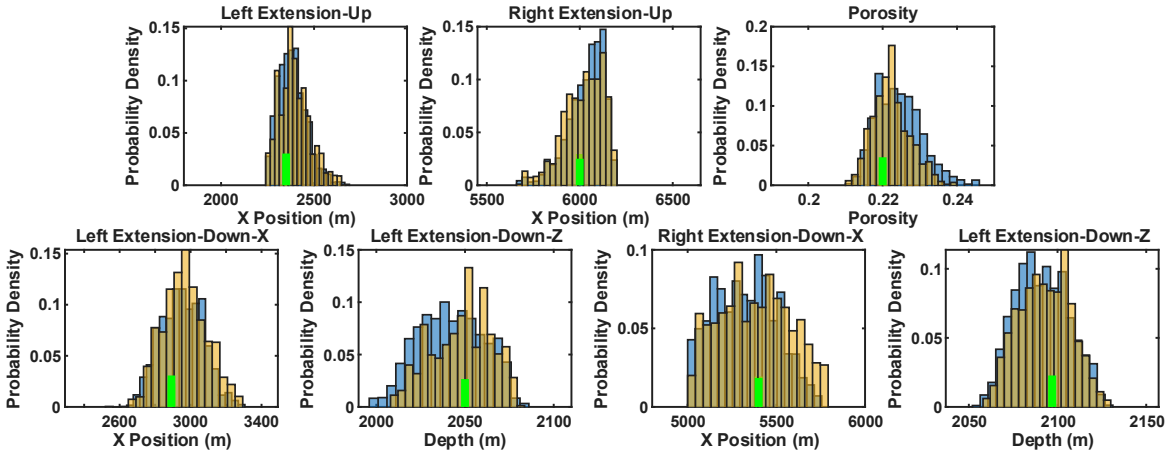


***Figure 2**. The results of FWI for two chains, each with 5,000 iterations, are illustrated in different colors. The green line represents the true value.*

CSEM inversion results: Using the seismic FWI–MCMC results, we treat the mean estimates as fixed inputs for the subsequent CSEM inversion. In contrast to seismic velocity, which typically exhibits a clear bulk change after CO_2 injection but limited sensitivity to within-plume saturation variations, the resistivity response is strongly saturation dependent. We considered a high-saturation zone near the injection well (distance ≈ 3200 m), followed by a linear decrease in saturation from about 3900 m to 5100 m, and finally a constant saturation at the right-hand side end of the plume (Figure 1b).

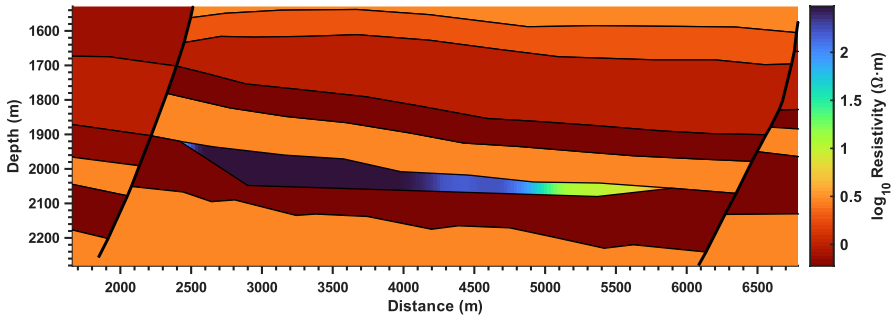


***Figure 3**. Zoomed-in reconstructed resistivity distribution of the study area.*

The inversion was performed using the amplitude and phase of the vertical electric field component. We ran the inversion for 15 iterations and achieved an adequate fit to the observed data. The recovered resistivity model in Figure 3 is consistent with the true resistivity and saturation distributions.

Conclusion

In this study, we presented a two-stage CO_2 monitoring workflow applied to a realistic homogeneous synthetic model of the Johansen Formation in the North Sea. The workflow first reconstructs plume geometry and porosity using probabilistic seismic FWI and then uses the resulting boundary to constrain a deterministic CSEM inversion for in-plume saturation. By incorporating saturation physics via Gassmann and Archie's relations and reconstructing the geometry and porosity using only seismic data, the approach reduces saturation-related non-uniqueness and enables stable, data-driven recovery of internal plume variability. The seismic FWI successfully reconstructed the geometry and porosity, including uncertainty quantification. The CSEM inversion achieved rapid misfit reduction, producing saturation and resistivity patterns consistent with the expected physical response, demonstrating the method's potential for uncertainty-aware plume delineation and quantitative storage assessment.

Acknowledgements

This work was supported by TotalEnergies E&P USA LLC and a grant from the Natural Sciences and Engineering Research Council of Canada (NSERC) [funding reference number 20220503].

References

Archie, G. E. (2003). The electrical resistivity log as an aid in determining some reservoir characteristics. *SPE reprint series*, 9-18.

Coreform Cubit (Version 2025.8) [Computer software]. Orem, UT: Coreform LLC. Retrieved from https://coreform.com

Gassmann, F. (1951). Uber die elastizitat poroser medien. *Vierteljahrsschrift der Naturforschenden Gesellschaft in Zurich*, *96*, 1-23.

Gassnova, 2012. In: Andfossen, P.O., Horntvedt, L., Ravn, T., Rørvik, K.L., Diesen, M., Keaney, G., Torgersen, T.A., Vetaas, M.V., Erichsen, E., Mohr, J. (Eds.), Geological Storage of CO2 from Mongstad. Interim Report Johansen Formation. Report TL02-GTL-Z-RA-0001.No. TL02-GTL-Z-RA-0001.

Hastings, W. K. (1970). Monte Carlo sampling methods using Markov chains and their applications. Biometrika 57, 1, p. 97–109.

Key, K. (2016). MARE2DEM: a 2-D inversion code for controlled-source electromagnetic and magnetotelluric data. *Geophysical Journal International*, *207*(1), 571-588.

Mackie, Randall L., and Theodore R. Madden. "Three-dimensional magnetotelluric inversion using conjugate gradients." *Geophysical Journal International* 115.1 (1993): 215-229.

Metropolis, N., Rosenbluth, A. W., Rosenbluth, M. N., Teller, A. H., & Teller, E. (1953). Equation of state calculations by fast computing machines. *The Journal of Chemical Physics*, *21*(6), 1087-1092.

Mosegaard, K., & Tarantola, A. (1995). Monte Carlo sampling of solutions to inverse problems. *Journal of Geophysical Research: Solid Earth*, *100*(B7), 12431-12447.

Ozah, R. C., Lakshminarasimhan, S., Pope, G. A., Sepehrnoori, K., & Bryant, S. L. (2005, October). Numerical simulation of the storage of pure CO2 and CO2-H2S gas mixtures in deep saline aquifers. In *SPE Annual Technical Conference and Exhibition?* (pp. SPE-97255). SPE.

Peter, D., Komatitsch, D., Luo, Y., Martin, R., Le Goff, N., Casarotti, E., ... & Tromp, J. (2011). Forward and adjoint simulations of seismic wave propagation on fully unstructured hexahedral meshes. *Geophysical Journal International*, *186*(2), 721-739.

Sundal, A., Nystuen, J. P., Rørvik, K. L., Dypvik, H., & Aagaard, P. (2016). The Lower Jurassic Johansen Formation, northern North Sea–depositional model and reservoir characterization for CO2 storage. Marine and Petroleum Geology, 77, 1376-1401.